Universal and nonuniversal neural dynamics on small world connectomes: A finite-size scaling analysis

Mahdi Zarepour,[1] Juan I. Perotti,[2] Orlando V. Billoni,[2] Dante R. Chialvo,[3] and Sergio A. Cannas[2]

[1]*Instituto de Física Enrique Gaviola, CONICET, Ciudad Universitaria, 5000 Córdoba, Córdoba, Argentina*

[2]*Facultad de Matemática, Astronomía, Física y Computación, Universidad Nacional de Córdoba, Instituto de Física Enrique Gaviola, CONICET, Ciudad Universitaria, 5000 Córdoba, Córdoba, Argentina*

[3]*Center for Complex Systems and Brain Sciences, Instituto de Ciencias Físicas, Universidad Nacional de San Martín, Campus Miguelete, 25 de Mayo y Francia, 1650 San Martín, Buenos Aires, Argentina*

(Received 5 June 2019; published 25 November 2019)

Evidence of critical dynamics has been found recently in both experiments and models of large-scale brain dynamics. The understanding of the nature and features of such a critical regime is hampered by the relatively small size of the available connectome, which prevents, among other things, the determination of its associated universality class. To circumvent that, here we study a neural model defined on a class of small-world networks that share some topological features with the human connectome. We find that varying the topological parameters can give rise to a scale-invariant behavior either belonging to the mean-field percolation universality class or having nonuniversal critical exponents. In addition, we find certain regions of the topological parameter space where the system presents a discontinuous, i.e., noncritical, dynamical phase transition into a percolated state. Overall, these results shed light on the interplay of dynamical and topological roots of the complex brain dynamics.

DOI: 10.1103/PhysRevE.100.052138

I. INTRODUCTION

The study of brain functional activity has revealed the existence of correlated fluctuations and scale invariance similar to those observed in critical phenomena. Such evidence prompted the conjecture that the large-scale organization of the brain emerges at criticality [1–3]. Despite the relevance of many of these findings, the small size of the available connectomes [4] does not allow one to determine whether the expected finite-size scaling behavior at criticality holds, as well as the associated universality class. In this work we study the dynamical properties of a model defined on a class of small world networks that share some topological features with the human connectome, for a wide range of values of the parameters that define the associated topology and for different system sizes. A finite-size scaling analysis allows not only for a robust characterization of criticality, but also for an estimation of critical exponents and therefore the identification of the universality class of the critical dynamics claimed to be relevant for the emergence of the large-scale organization of brain activity. Since finite-size scaling is a central issue in the description of critical phenomena, the present results provide a necessary perspective about the expected scaling behaviors on previous human-connectome-based models which predict brain dynamics consistent with any kind of criticality [4–8].

The paper is organized as follows. In Sec. II we describe the model as well as the simulation and finite-size scaling methods used. The results are presented in Sec. III. We discuss the relevance of the main findings in Sec. IV.

II. MODEL AND METHODS

A. Model

This work uses an adaptation of the neural model presented in Ref. [4] running over a small-world network with a weighted adjacency matrix w_{ij}. To mimic the weight distribution of the human connectome [4,9], the non-null w_{ij} are chosen randomly from an exponential distribution $p(w) = \lambda e^{-\lambda w}$, with $\lambda = 12.5$. This gives a good fitting of the available connectome data.

The node dynamics of the neural model respond to the Greenberg-Hastings cellular automaton [10], in which each node i of the network is associated with a three-state variable $x_i = 0, 1, 2$, corresponding to the following dynamical states: the quiescent ($x_i = 0$), excited ($x_i = 1$), and refractory ($x_i = 2$) states. The transition rules are as follows. If a node at the discrete time t is in the quiescent state $x_i(t) = 0$ it can make a transition to the excited state $x_i(t+1) = 1$ with a small probability r_1 or if $\sum_j w_{ji}\,\delta(x_j(t), 1) > T$, where T is a threshold and $\delta(x, y)$ is a Kronecker delta function, then $x_i(t+1) = 0$. If it is excited $x_i(t) = 1$, then it becomes refractory $x_i(t+1) = 2$ always. If it is refractory $x_i(t) = 2$, then it becomes quiescent $x_i(t+1) = 0$ with probability r_2 and remains refractory $x_i(t+1) = 2$ with probability $1 - r_2$. Following Ref. [4], we set $r_1 = 10^{-3}$ and $r_2 = 0.3$.[1] We keep these values fixed in all the calculations. Each node interacts

[1]We made several checks for different values of $r_2 \sim 10^{-1}$ and no qualitative differences were observed.

with the others according with the topology of a small-world network, constructed as the usual Watts-Strogatz (WS) model [11]. That is, we start from a ring of N nodes in which each node is connected symmetrically to its $2m$ nearest neighbors. Then, for each node each vertex connected to a clockwise neighbor is rewired to a random node with probability π and preserved with probability $1-\pi$, so the average degree $\langle k\rangle = 2m$ is preserved [12].

B. Statistical properties

The present analysis focuses on the dynamical clusters of coherent activity, namely, groups of nodes simultaneously activated ($x_i = 1$) which are linked through nonzero weights w_{ij}, for different values of the parameters (π, $\langle k\rangle$) and different network sizes N. Each simulation started from a random distribution of activated sites and we let the system run 100 time steps before starting to collect data. We found that time interval to be enough for the system to reach a stationary state for any system size and for any value of the network parameters. Then we recorded data every five time steps, to avoid artifactual correlation effects. For each data set we computed several measures to describe a percolationlike critical phenomenon as a function of the control parameter T [4]. Specifically, we calculated the average sizes of the largest, i.e., giant, cluster $\overline{S}_1$, which can be considered the order parameter, and we also computed the average size of the second largest cluster $\overline{S}_2$, together with the average cluster size

$$\langle s\rangle = \frac{\sum_s' s^2 N_s}{\sum_s' s N_s}, \tag{1}$$

where the primed sum runs over all cluster sizes except the giant one and N_s is the number of clusters of size s [12,13]. In some cases we also computed the cumulative complementary distribution function (CCDF) of cluster sizes. Depending of the case, averages were computed both over data obtained along the same simulation run and over different networks.

If the system presents a percolationlike critical point, both $\langle s\rangle$ and $\overline{S}_2$ are expected to exhibit a (size-dependent) maximum for a certain pseudocritical value of the control parameter (the threshold T in the present case) that scales with the system size as [14] $\langle s\rangle \sim N^{\gamma/\nu d}$ and $\overline{S}_2 \sim N^{d_f/d}$. Here γ and ν are the standard susceptibility and correlation length critical exponents, respectively. In addition, d is the effective dimension of the system, namely, it equals the spatial dimension D if $D < d_c$ (d_c being the upper critical dimension) and it equals d_c otherwise. The latter applies in the present case since it is known that the global dimension of a WS graph is always infinite [15]. Further, d_f is the fractal dimension of the percolating cluster. Also at the critical point it is expected that [14] $P(s) \sim s^{-\tau}\exp(-s/S^*)$, where $S^* \propto \overline{S}_2$.

III. RESULTS

As already mentioned, the distribution of cluster sizes of activity can be informative of the different dynamical regimes of the model. We computed such measures as a function of the threshold T for models of increasing sizes N and different topologies by varying the average degree $\langle k\rangle$ and rewiring π. The model dynamics can be explored by inspecting the clusters' finite-size scaling behavior as a function of these three parameters. Figures 1–3 correspond to the three typical behaviors found at well-defined regions in parameter space, which we will describe in detail now.

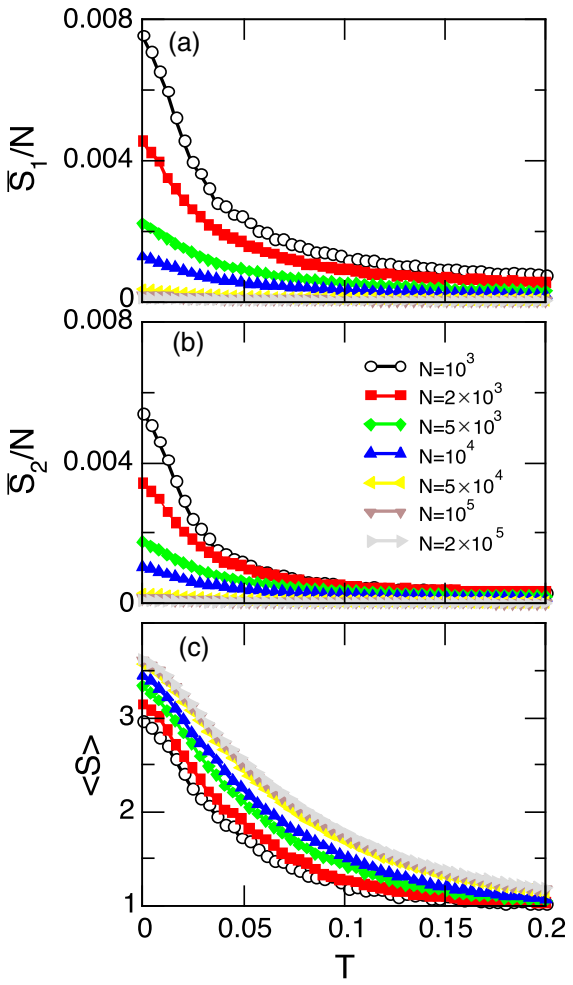

FIG. 1. Finite-size behavior for $\pi = 0.6$ and $\langle k\rangle = 5$ corresponding to the segregated regime of the model where phase transition is absent for any T. (a) Order parameter $\overline{S}_1/N$. (b) Second largest cluster relative sizes. Notice that they are of the same order of magnitude as the largest clusters shown in (a) and also that $\overline{S}_2/N \to 0\,\forall\, T$ when $N \to \infty$. (c) Average clusters size $\langle s\rangle$ as a function of the threshold T for different sizes N.

At relatively low average degree $\langle k\rangle$, the example of Fig. 1 is typical. We see that $\overline{S}_1/N$ goes to zero for any value of T as $N \to \infty$. Also, both $\overline{S}_2/N$ and $\langle s\rangle$ display a monotonic decrease (no peak) for any value of the system size N. Thus, for those small-world topologies only a few small and uncorrelated clusters are present at any time for any value of the threshold T, resembling what Tononi *et al.* [16] describe as a *segregated* regime, which *per se* is incompatible with normal brain functioning. Increasing the value of $\langle k\rangle$ results in a change of the model dynamics. For such a case, as shown in Fig. 2, the cluster analysis reveals the characteristic finite-size scaling behavior exhibited by percolation phenomena [14]. There we observe the existence of a critical threshold T_c below which the order parameter converges to a finite value when $N \to \infty$, while it goes to zero above the critical threshold

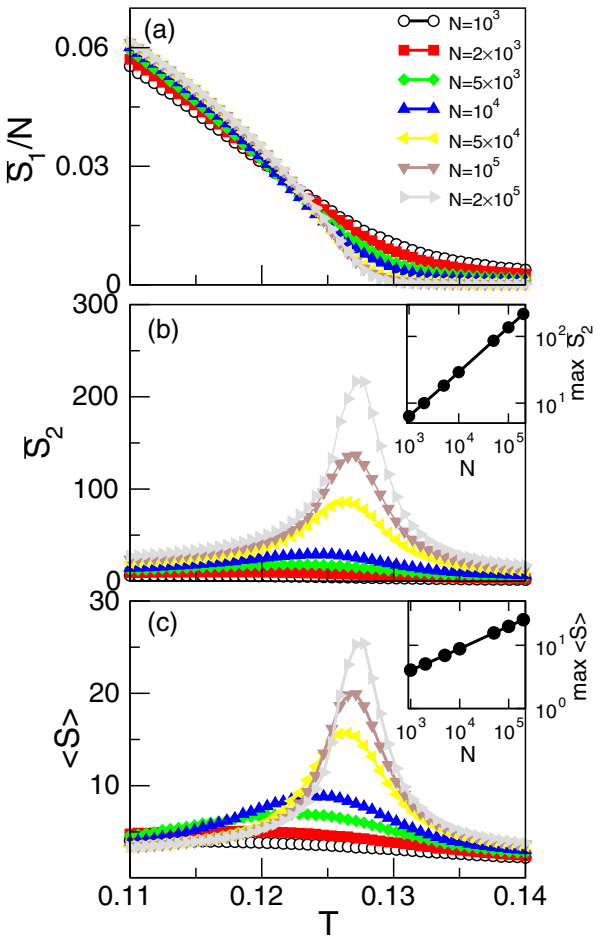

FIG. 2. Finite-size behavior for $\pi = 0.6$ and $\langle k \rangle = 10$, corresponding to the critical regime (MFC). (a) Order parameter. (b) Second largest cluster size $\overline{S}_2$. The inset shows the maximum of $\overline{S}_2$ as a function of N, where the solid line is a power-law fitting giving a critical exponent $d_f/d = 0.67 \pm 0.02$. (c) Average clusters size $\langle s \rangle$. The inset shows the maximum of $\langle s \rangle$ as a function of N, where the solid line is a power-law fitting giving a critical exponent $\gamma/\nu d = 0.35 \pm 0.02$.

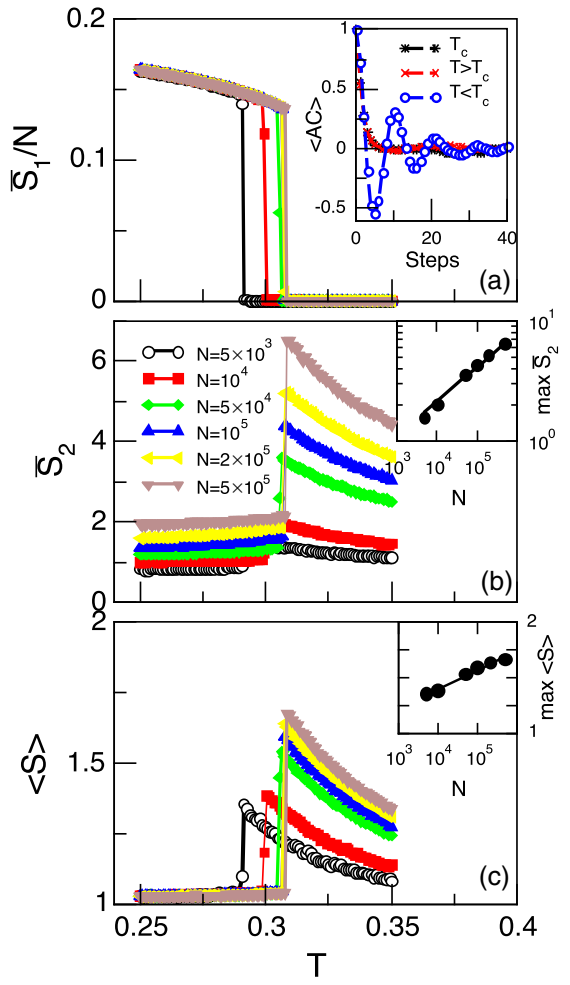

FIG. 3. Finite-size behavior for $\pi = 0.6$ and $\langle k \rangle = 30$, corresponding to the discontinuous regime. (a) Order parameter. The inset shows the autocorrelation function of the average total activity AC close to the critical value T_c. (b) Second largest cluster size $\overline{S}_2$. The inset shows the maximum of $\overline{S}_2$ as a function of N, where the solid line is a power-law fitting giving a critical exponent $d_f/d = 0.29 \pm 0.02$. (c) Average clusters size $\langle s \rangle$. The inset shows the maximum of $\langle s \rangle$ as a function of N, where the solid line is a power-law fitting giving a critical exponent $\gamma/\nu d = 0.05 \pm 0.02$. The inset shows the autocorrelation function of the average activity for three values of T very close to T_c.

[Fig. 2(a)]. This means the existence of a dynamical phase transition, where the system develops long-range order in the form of a macroscopic correlated cluster of simultaneously active nodes, which resembles the correlations associated with the brain resting state networks (RSNs) described in [4]. Also both $\overline{S}_2$ and $\langle s \rangle$ exhibit a sharp peak around $T = T_c$ [see Figs. 2(b) and 2(c)] that diverges as a power law when $N \to \infty$, thus exhibiting well-defined critical exponents. Hence, for the associated topologies, the dynamical phase transition is indeed a second-order or critical one.

A very different transition happens for large enough values of both parameters $(\pi, \langle k \rangle)$. Indeed, in that region both the order parameter and the fluctuation measures $\overline{S}_2$ and $\langle s \rangle$ exhibit an apparently discontinuous behavior at the transition point, as illustrated in Fig. 3.

By analyzing the finite-size scaling of any of the three quantities $\overline{S}_1/N$, $\overline{S}_2$, and $\langle s \rangle$ in the large-N limit we estimated the frontiers in the $(\pi, \langle k \rangle)$ space between the regions where the system may or may not exhibit a dynamical phase transition, as well as the nature of the transition (see Fig. 4). The frontier between the segregated and mean-field critical (MFC) regimes was obtained by analyzing whether there is a $T_c > 0$ such that $\overline{S}_1/N$ converges to a finite value for $T < T_c$ when $N \to \infty$. The frontier between the MFC and nonuniversal critical (NUC) regimes was identified by analyzing whether or not the difference between critical exponents $\gamma/\nu d$ and d_f/d (obtained from the finite size scaling extrapolation) and the corresponding percolation mean-field values exceeds the associated error bars. The frontier between the NUC and oscillatory regimes was estimated by analyzing whether or not there is a discontinuity in the order parameter at the transition in the large-N limit.

At relatively low average degree $\langle k \rangle$ there is no transition (the region labeled NT in Fig. 4). When present, the nature of

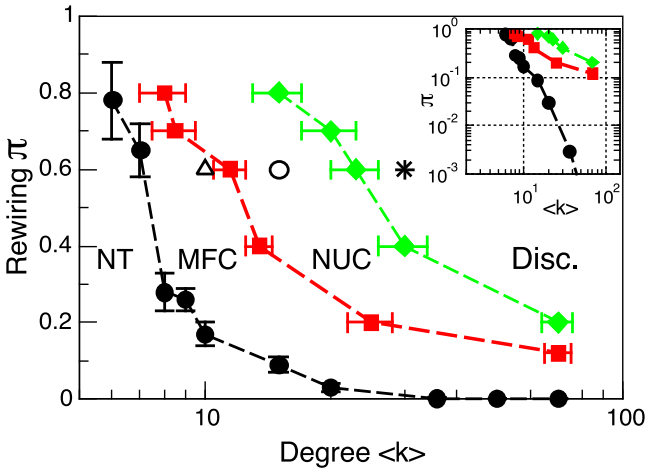

FIG. 4. Parameter space for the network topology values $(\pi, \langle k \rangle)$ in the large-N limit. As a function of the node threshold T, the system can exhibit a percolationlike dynamical phase transition for parameter values above the black line. Below the black line there is no dynamical phase transition (NT). Between the black line and the red dashed line (MFC) the behavior becomes scale invariant, at a certain critical threshold T, with exponents consistent with the mean-field percolation universality class. Farther above, in the region denoted by NUC, the behavior can be still scale invariant and critical, i.e., the transition is still second order, but without universal exponents. Finally, above the green dash-dotted line, the transition becomes discontinuous (Disc.) and the dynamic is short-range correlated and oscillatory. The triangle, circle, and star at $\pi = 0.6$ correspond to the parameter values used for the statistics presented in Figs. 5(a), 5(b), and 5(c), respectively. In the inset the same data are plotted in on a double logarithmic axis to best denote the relative sizes of each dynamical regime.

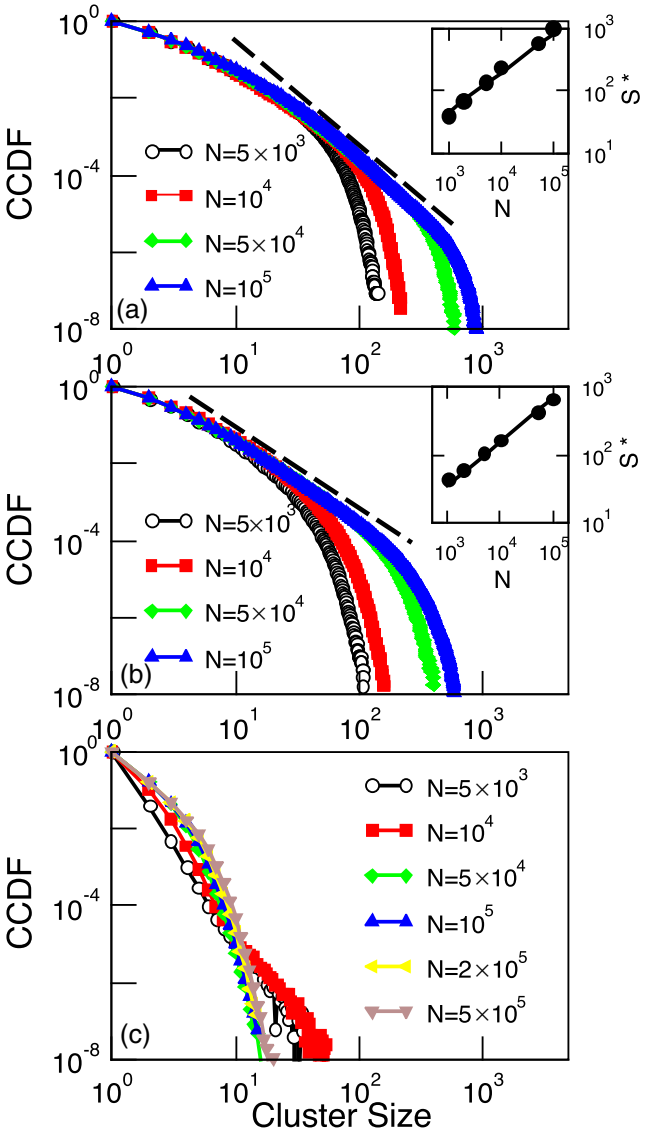

FIG. 5. (a) The CCDF of the cluster size distribution for $\langle k \rangle = 10$, $\pi = 0.6$, and different system sizes. The dashed line corresponds to a linear fitting of the central part of the distribution with a power law $\sim s^{-1.58}$. The inset shows the cutoff S^* as a function of N; the solid line is a power-law fitting giving an exponent 0.62 ± 0.05. (b) The CCDF of the cluster size distribution for $\langle k \rangle = 15$, $\pi = 0.6$, and different system sizes. The dashed line corresponds to a linear fitting of the central part of the distribution with a power law $\sim s^{-1.54}$. The inset shows the cutoff S^* as function of N; the solid line is a power-law fitting giving an exponent 0.60 ± 0.03. (c) The CCDF of the cluster size distribution for $\langle k \rangle = 30$, $\pi = 0.6$, and different system sizes.

the dynamical phase transition can be different depending on the topology of the network, as depicted in Fig. 4.

For relatively small values of $\langle k \rangle$ and/or small enough values of π, the behavior is critical and the corresponding critical exponents are consistent with the universality class of mean-field (or Bethe) classical percolation, namely, $\gamma/\nu d \approx 1/3$ and $d_f/d = 2/3$ (corresponding to an upper critical dimension $d = 6$, $d_f = 4$, $\nu = 1/2$, and $\gamma = 1$). An example is the case shown in Fig. 2.

To get further insight into the nature of the dynamical phase transition in the previously mentioned region, we analyzed the associated behavior of the cluster size distribution (see Fig. 5). For the critical dynamics, consistently, the cumulative cluster size distribution exhibits the expected behavior $P_c(s) \equiv \sum'_{s' \geqslant s} P(s') \sim s^{-(\tau-1)} \exp(-s/S^*)$, with an exponent $\tau \approx 5/2$ and $S^* \propto \overline{S}_2$ (thus satisfying the scaling law $\tau = d/d_f + 1$) as shown in Fig. 4, corresponding to the region in the $(\pi, \langle k \rangle)$ space denoted by MFC.

For even larger values of π and/or $\langle k \rangle$, a wide region of the parameter space results in critical exponents changing continuously with the topological parameters, until they seem to saturate (see Fig. 6). On the other hand, the power-law increase of values of $\overline{S}_2$ [see Fig. 3(b)] at both sides of the discontinuity with an exponent close to $1/3$ implies a roughly two-dimensional percolating cluster ($d_f \approx 2$), assuming an effective dimension $d = 6$.

For comparison, we also calculated the clusters size distribution for a set of values in the NUC region, as shown in Fig. 5(b). The power-law distribution is indeed consistent with critical behavior. On the other hand, the data in Fig. 5(c) show that the cluster size distribution for large values of $(\pi, \langle k \rangle)$, for large enough system sizes ($N > 10^4$), exhibits an

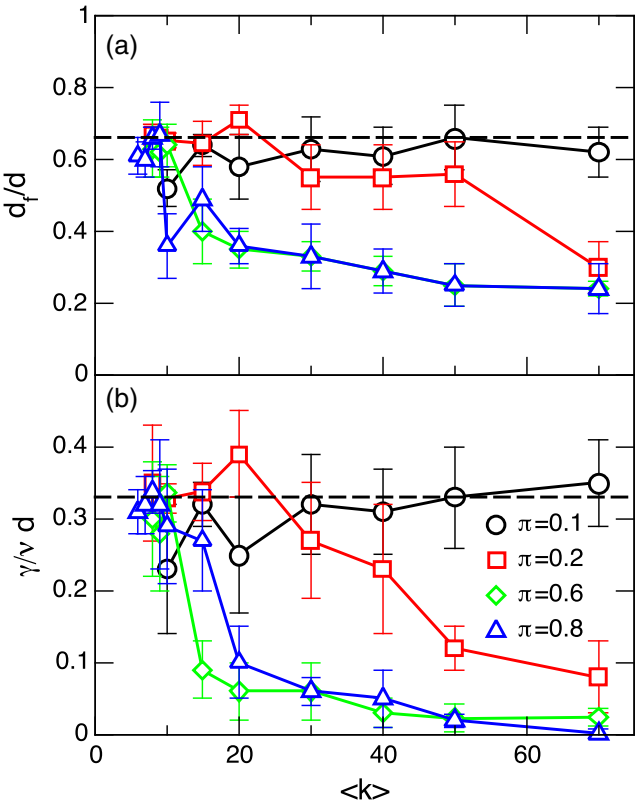

FIG. 6. Critical exponents obtained by finite-size scaling analysis as a function of $\langle k\rangle$ for the range of the rewiring probability π values given in the legend. (a) Critical exponent of the maximum of $\overline{S}_2$. The dashed line corresponds to the mean-field value $d_f/d = 2/3$. (b) Critical exponent of the maximum of $\langle s\rangle$. The dashed line corresponds to the mean-field value $\gamma/\nu d \approx 1/3$.

exponential decay, which excludes critical behavior. Hence, we can conclude that in such a region the system exhibits a first-order or discontinuous dynamical percolation transition. In this region the analysis of the autocorrelation function of the mean activity [see the inset in Fig. 3(a)] reveals that the dynamics exhibits a finite timescale corresponding to an oscillation whose period is a function of the topological parameters π and $\langle k\rangle$ as well as T.

The results of the scaling analysis are summarized in Fig. 6, which shows the computed critical exponents both for the maximum of $\overline{S}_2$ [Fig. 6(a)] and for the maximum of $\langle s\rangle$ [Fig. 6(b)]. The data show the two behaviors already discussed: the universal (mean field, denoted by closed circles) and that for the cases in which there is a continuously changing exponent depending on the value of π.

IV. DISCUSSION

The main results of the present work illustrate how the large-scale correlated activity depends on the topological details of the underlying structural network. The results show that the correlated patterns exhibiting scale invariance seen in the brain RSNs need a certain minimum of connectivity conditions. In other words, using the terminology of Tononi *et al.* [16], for relatively low average degree $\langle k\rangle$ and fraction of network shortcuts π, the neuronal activity is too segregated. In the other extreme, for very large values of $\langle k\rangle$ and π, the activity is too integrated, exhibiting a first-order or discontinuous phase transition. This is most unexpected, because in conventional static percolation on small-world networks the transition is second order, belonging to the mean-field universality class for any value of the rewiring probability π [17]. Hence, the present effect is due entirely to dynamical correlations. In between these two extremes we found a regime that seems compatible with the functional magnetic resonance imaging brain data. There, two different dynamical regimes are found which are characterized by different kinds of dynamical phase transitions as the threshold controlling the neuronal activation is varied. For certain values the phase transition is universal and for other, larger values, while the scale invariance persists, the universality is lost, i.e., the exponents change continuously. Such regions could correspond, with some differences, to the equivalent to the Griffiths phases [18] already described in another context [19,20]. We refer the reader to some recent results in the context of the brain connectome [21,22].

It is worth noting the presence of standard percolation critical exponents, considering that this kind of dynamical phase transition could be expected to belong to the directed percolation (DP) universality class [23]. Just for comparison, the mean field DP exponents are [24] $\gamma/\nu d = d_f/d = 1/2$ (which come from $\gamma = 1$, $\beta = 1$, $\nu = 1/2$, and the hyperscaling relation $d_f = d - \beta/\nu$, with an upper critical dimension $d = 4$). The reasons for the absence of DP critical exponents in the present case are not clear. Among the possibilities are disorder [25] and the presence of a spontaneous activation probability r_1, which rules out the possibility of an absorbing inactive state, considered a main property needed to observe the DP universality class [23].

From the neuroscience point of view, the relevant finding is that the critical regime in this class of networks spans a wide region in the parameters space, corresponding to intermediate values of networks topologies; those that are too connected or too disconnected are not able to exhibit critical dynamics, regardless of the values of the other two parameters (system size and the node's threshold). In other words, from the point of view of neural architecture, a minimum of connectivity needs to be predetermined (perhaps via evolution) in order for the dynamics to achieve the dynamical features of criticality (via modulation of excitability or the threshold). On the other hand, the discontinuous percolation that appears only for extremely connected networks might constitute pathological conditions observed in real nervous systems. Hence, critical fluctuations emerge as a robust characteristic of variations in the anatomical network topology, which is consistent with the expectations of criticality described for the spontaneous fluctuations of brain dynamics.

It is well known that Watts-Strogatz networks are too short to describe all the features of the interactions of real brains, such as modular structure and topological dimensionality. Nonetheless, the present results show that even in the absence of such higher-order features of the interactions there is a rich diversity of dynamics. Future work should shed light on the impact over the dynamics when such higher-order properties of the interaction graph are included.

ACKNOWLEDGMENTS

This work was partially supported by CONICET (Argentina) through Grant No. PIP 11220150100285, Ministerio de Ciencia y Tecnología de la Provincia de Córdoba (Argentina) through Grant No. PID2018, SeCyT (Universidad Nacional de Córdoba, Argentina), and NIH (U.S.) Grant No. 1U19NS107464-01. M.Z. was a recipient of a Doctoral Fellowship from CONICET (Argentina). This work used Mendieta Cluster from CCAD-UNC, which is part of SNCAD-MinCyT, Argentina.

[1] J. M. Beggs and D. Plenz, J. Neurosci. **23**, 11167 (2003).
[2] D. R. Chialvo, Nat. Phys. **6**, 744 (2010).
[3] T. Mora and W. Bialek, J. Stat. Phys. **144**, 268 (2011).
[4] A. Haimovici, E. Tagliazucchi, P. Balenzuela, and D. R. Chialvo, Phys. Rev. Lett. **110**, 178101 (2013).
[5] G. Deco and V. K. Jirsa, J. Neurosci. **32**, 3366 (2012).
[6] G. Deco, M. Senden, and V. K. Jirsa, Front. Comput. Neurosci. **6**, 68 (2012).
[7] D. Marinazzo, M. Pellicoro, G. Wu, L. Angelini, J. M. Cortes, and S. Stramaglia, PLoS One **9**, e93616 (2014).
[8] S. Stramaglia, M. Pellicoro, L. Angelini, E. Amico, H. Aerts, J. M. Cortes, S. Laureys, and D. Marinazzo, Chaos **27**, 047407 (2017).
[9] P. Hagmann, L. Cammoun, X. Gigandet, R. Meuli, C. J. Honey, V. J. Wedeen, and O. Sporns, PLoS Biol. **6**, e159 (2008).
[10] J. M. Greenberg and S. P. Hastings, SIAM J. Appl. Math. **34**, 515 (1978).
[11] D. J. Watts and S. H. Strogatz, Nature (London) **393**, 440 (1998).
[12] A. Barrat, M. Barthelemy, and A. Vespignani, *Dynamical Processes on Complex Networks* (Cambridge University Press, Cambridge, 2008).
[13] A. Margolina, H. J. Herrmann, and D. Stauffer, Phys. Lett. A **93**, 73 (1982).
[14] D. Stauffer and A. Aharony, *Percolation Theory* (Taylor & Francis, London, 2003).
[15] M. E. J. Newman and D. J. Watts, Phys. Rev. E **60**, 7332 (1999).
[16] G. Tononi, O. Sporns, and G. M. Edelman, Proc. Natl. Acad. Sci. USA **91**, 5033 (1994).
[17] C. Moore and M. E. J. Newman, Phys. Rev. E **62**, 7059 (2000).
[18] R. B. Griffiths, Phys. Rev. Lett. **23**, 17 (1969).
[19] M. A. Muñoz, R. Juhász, C. Castellano, and G. Ódor, Phys. Rev. Lett. **105**, 128701 (2010).
[20] P. Moretti and M. A. Muñoz, Nat. Commun. **4**, 2521 (2013).
[21] G. Ódor, Phys. Rev. E **94**, 062411 (2016).
[22] G. Ódor, Phys. Rev. E **99**, 012113 (2019).
[23] H. Hinrichsen, Adv. Phys. **49**, 815 (2000).
[24] H. K. Janssen and U. C. Tauber, Ann. Phys. (NY) **315**, 147 (2005).
[25] S. R. Dahmen, L. Sittler, and H. Hinrichsen, J. Stat. Mech. (2007) P01011.